ELSEVIER

Journal of Nuclear Materials 241–243 (1997) 255–259

journal of nuclear materials

Erosion lifetime of ITER divertor plates

H.D. Pacher [a,*], I. Smid [a], G. Federici [b], Yu. Igitkhanov [b], G. Janeschitz [b], R. Raffray [b], G. Vieider [a]

[a] *The NET Team, Garching JWS, D-85748 Garching, Germany*
[b] *ITER Joint Central Team, Garching JWS, D-85748 Garching, Germany*

Abstract

For ITER divertor operation in the detached regime, erosion of divertor plates made of beryllium, carbon fibre composites and tungsten–rhenium alloys is evaluated. Erosion due to (a) physical and, for CFC, chemical sputtering (including surface temperature variation over the lifetime because of neutron irradiation), (b) disruption thermal quench using published data and (c) evaporation and melt layer loss (metals) for infrequent high-power transients (20 MW/m^2, up to 10 s) is evaluated both with and without the reduction of net incident power by radiation from the evaporated impurities ('low density vapour shield'). The composite lifetime is calculated for normal operation (detached, 10% transients, 10% disruptions); the effect of an increase in transient frequency and in incident power (semi-attached operation) is determined. The resulting erosion lifetime excludes beryllium, whereas both CFC and W–3%Re yield acceptable lifetimes.

Keywords: ITER; Impurity source; Physical erosion; Chemical erosion; Erosion and particle deposition; Fusion technology

1. Introduction

The erosion lifetime of the ITER divertor plates is determined by three main processes: sputtering (physical and chemical), disruption erosion and slow transients. ITER is assumed to operate in the detached regime described in Ref. [1] i.e. at a nominal power load of 5 MW/m^2. For the basic performance phase, it is assumed that 1 shot of 10 has a slow transient lasting up to 10 s and that 1 shot of 10 ends in a disruption.

Previous estimates of the divertor erosion lifetime are found in Refs. [2–6] and references therein. In the present work, the lifetime is estimated for three candidate materials: beryllium, Dunlop carbon fibre composite (CFC) and tungsten–3%-rhenium alloy (W3Re); their properties are given in more detail in Ref. [4]. The actual tile geometry is used: flat tile for Be and W3Re, monobloc for CFC. For CFC, the progressive degradation of thermal conductivity with irradiation [7] is taken into account. Furthermore, the effect on lifetime of an increase in the frequency of slow transients and of an increase in the nominal power is considered.

2. Sputter erosion

Physical sputtering is evaluated using the yields of Ref. [8], taking 1 as the angle enhancement factor and assuming ions with a shifted Maxwellian distribution having an average energy $4T_e$ (these values agree with JET results). D, T and He are assumed to impinge on the walls in the ratio 0.5:0.5:0.2. Self-sputtering and impurities other than He are not considered. For nominal steady-state operation, the power on the divertor plate is assumed to be 2.5 MW/m^2 in ions and the same in radiation; the power on the side walls is taken to be 0.5 MW/m^2, carried by neutrals of average energy $2T_n$. At the divertor plates, redeposition is assumed to be 90% (in Ref. [9], a detailed calculation gave net and gross erosion rates of 3 and 63 nm/s, respectively, i.e. 95% redeposition). No local redeposition is assumed at the side walls.

* Corresponding author. Tel.: +49-89 3299 4293; fax: +49-89 3299 4312; e-mail: pacher@ipp-garching.mpg.de.

PII S0022-3115(96)00510-7

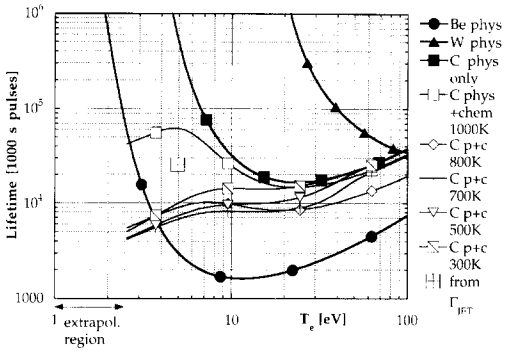

Fig. 1. Sputter lifetime of target for ion impact for characteristic thicknesses (Be: 1 cm, W: 1 cm, C: 3 cm); physical and chemical (carbon, as $\Gamma^{-0.22}$) sputtering included. $Q = 2.5$ MW/m^2 90% redeposition, angle factor = 1, $\langle E \rangle = 4kT_e$, D:T:He = 0.5:0.5:0.2.

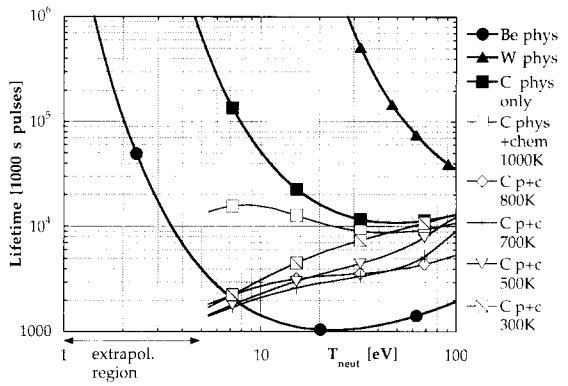

Fig. 2. Sputter lifetime of target for neutral impact for characteristic thicknesses (Be: 1 cm, W: 1 cm, C: 3 cm); physical and chemical (carbon, as $\Gamma^{-0.22}$) sputtering included. $Q = 0.5$ MW/m^2, no redeposition, $\langle E \rangle = 2kT_{neutral}$.

Chemical sputtering for carbon is evaluated using the formulas of Ref. [10]. However, the dependence on incident flux (as $\Gamma^{-0.1}$ for the 'thermal' term and independent for the 'athermal' term in Ref. [10]) appears to be too weak to explain results from tokamak target plates. In particular, DITE and Tore Supra find the chemical sputtering to be weaker and JET [11] found that a yield of 0.2%, a factor 10 below expected, corresponds to global modelling (an indirect procedure). More recently JET [12] found by CII measurements that the sputtering yield for a 10 eV shot could be explained by physical sputtering alone and was a factor 4 below that predicted for chemical and physical sputtering. This reduced chemical sputtering case is estimated by assuming both terms of Ref. [10] to vary as $\Gamma^{-0.22}$, a conservative value from the experimental results in tokamaks. More recent formulas showing the same trend [13] will be applied in the future.

The resulting sputter lifetime is given in Fig. 1 for the target, for representative thicknesses of the material (varied below). In the range of $T_e = 3$–10 eV, the sputter lifetime at the target is seen to be low for beryllium, good for CFC, and very good for W (in the absence of impurities other than He). These results are the basis for the composite lifetime estimate, using for CFC the actual surface temperature over the life.

The lifetime at the divertor side wall and lower baffle (Fig. 2) for neutral impact at 0.5 MW/m^2 and expected neutral temperatures of several tens of eV, is too low for both Be and CFC, since components such as the baffle are not to be exchanged as frequently as the divertor plates. Tungsten is therefore the preferred plasma-facing material for the side walls and lower baffle.

3. Disruption erosion

The erosion due to the thermal quench of disruptions has been modelled in Refs. [14–16] (see also Ref. [17]). Evaporation, finite rate ionisation/ recombination, radiation and radiation transport are taken into account in Refs. [14–16]. The high density vapour shielding produced by evaporation of the surface is found to reduce strongly the energy incident on the plate. To estimate the remaining erosion, typical results from this work (2D results, now becoming available, are not yet included) are plotted in Fig. 3, as is also the melt depth for the metals (Be or W–3%Re). In the absence of models confirmed by experiment, we assume here that either 10% or 50% of this melt layer is lost on average. For disruptions depositing 100 MJ/m^2, the loss is then 30 μm per event for CFC. For both Be and W, the loss (evaporation and 10% or 50% melt layer loss) is 23 or 75 μm per event, respectively.

We note that, for frequent ELMs, surface melting and strong evaporation must be avoided. A separate analysis has shown that the energy per ELM must remain below 0.5 to 1 MJ/m^2 for CFC and 1/3 this value for Be.

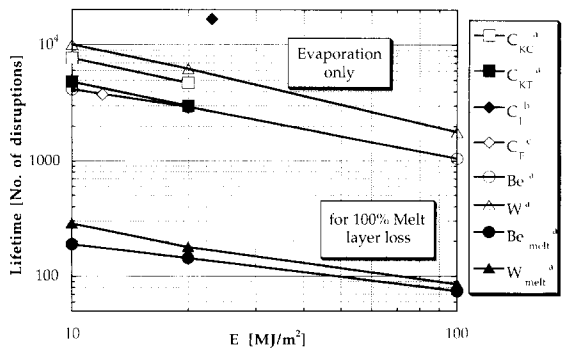

Fig. 3. Disruption lifetime for representative thickness (Be: 1 cm, W: 1 cm, C: 3 cm), including vapour shielding, from (a) Ref. [14], (b) Ref. [15] and (c) Ref. [16]. Actual melt layer loss assumed to be 10 to 50% of this (see text).

4. Erosion by slow transients

For divertor plates dimensioned for a nominal 5 MW/m^2 in detached operation, infrequent slow transients of attached operation (typically 20 MW/m^2 for 10 s, once every 10 shots) yield strong surface evaporation (CFC and metals) and melting (metals only). During the transient, the power heating the plate is reduced by evaporation cooling and black-body radiation. It could be further reduced by impurity radiation near the plate once the impurities released there are ionised. This 'low-density vapour shield'was estimated in Ref. [18], but a dedicated experiment in JET [19] showed this effect to be very small. In shots without gas puff, less than 5% of the Be neutral flux evaporated was ionised, Be radiation levels remained low and severe melting ensued. The observed melt layer loss was 3 mm (toroidally uniform) in 5 high-power shots i.e. 25% of the expected melt layer (2.4 mm for this case) per event.

The response of the divertor plates to these transients is calculated with and without the 'low-density vapour shield' in full 2D geometry (see Refs. [4,18,20]).

5. Composite lifetime

The maximum thickness of the divertor tiles is determined by imposing a maximum surface temperature in normal operation (5 MW/m^2) of 1080 K for Be and 1780 K for CFC and W–3%Re. The minimum thickness is taken to be 2 mm (assuming adequate cooling can be provided, since otherwise a large fraction of the potential lifetime would be unused). The remaining thickness as a function of the number of shots is given in Fig. 4 and the thicknesses and lifetimes are given in Table 1. Whereas the results with vapour shield during transients are also quoted,

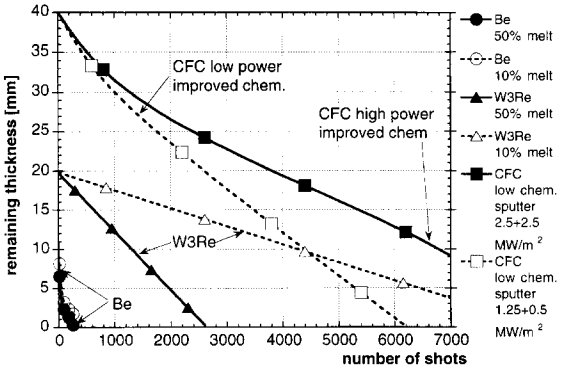

Fig. 4. Remaining thickness versus shots for CFC (improved chemical sputtering, two points in power profile, see text), and metals (Be and W–3%Re, 2 values of melt loss).

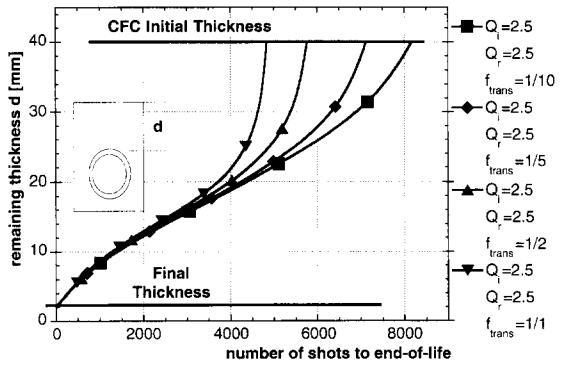

Fig. 5. Remaining CFC thickness versus shots to end-of-life for different frequencies of slow transients (1 shot in every 10, 5, ... 1 shots) for peak power point, attached operation and reduced chemical sputtering (see text).

Table 1
Lifetime in basic performance phase. 90% redeposition, 10% slow transients and 10% disruptions

	Initial thickness (mm)	Final thickness (mm)	Lifetime with transient vapour shield	Without transient vapour shield			
				transients (mm)	disruptions (mm)	sputter (mm)	shots
Be 50% melt	11	2	(570)	7.5	0.9	0.6	**120**
Be 10% melt	11	2	(1010)	7.3	0.5	1.2	**225**
W3Re 50% melt	20	2	(2400)	0.3	17.7	<	**2370**
W3Re 10% melt	20	2	(7820)	0.2	17.8	<	**7740**
C $G-R/R$ [a,c]	40	2	(9330)	(8.7)	(20.9)	(8.4)	(6970)
C $G-R/R$ [b,c]	40	2	(2410)	(3.6)	(6.1)	(28.3)	(2020)
C $\Gamma^{-0.22}$ [a,c]	40	2	(10490)	8.7	24.6	4.7	**8170**
C $\Gamma^{-0.22}$ [b,c]	40	2	(7120)	6.6	17.6	13.8	**5840**

[a] High power, $Q_{ion} = 2.5$ MW/m^2 and $Q_{rad} = 2.5$ MW/m^2.
[b] Low power, $Q_{ion} = 1.25$ MW/m^2 and $Q_{rad} = 0.5$ MW/m^2.
[c] Values $G-R/R$ too pessimistic; use values with flux dependence as $\Gamma^{-0.22}$ (see text).

Table 2
Input conditions for variable power calculation

Nominal power (MW/m^2)	Thickness (mm)			Particles (MW/m^2)		Radiation (MW/m^2)		T_e (eV)
	Be	CFC	W–3%Re	peak	low power	peak	low power	
5.0	11.7	40.0	20.0 [a]	2.5	1.25	2.5	0.5	4
7.5	6.5	23.5	17.5	5.5	3.0	2.0	0.5	6
10.0	4.1	15.7	12.4	9.0	4.5	1.0	0.5	8
20.0	0.8 [b]	7.3 [c]	5.0	20	10	0	0	15

[a] 20 mm rather than 28.5 (see text).
[b] 20 MW/m^2 not possible for Be.
[c] Unirradiated since lifetime short at 20 MW/m^2.

in view of Ref. [18] only the values without mitigating impurity radiation (last column of Table 1) are considered for the design.

For CFC, the variation in surface temperature over the life, which affects both the evaporation by slow transients and the chemical sputtering, includes the change in thermal conductivity by neutron irradiation. The high-power point quoted is at nominal power, the low-power point (1.25 MW/m^2 in particles, 0.5 in radiation) has lower power, lower temperature, higher chemical sputtering and therefore lower lifetime.

Note that Be lifetimes are dominated by slow transients, CFC lifetimes are influenced by all three processes and W3Re lifetimes are dominated by disruptions (see also Section 6).

Be lifetimes are inadequate. Both CFC and W3Re yield acceptable lifetimes, much more than 1000 shots. Since a low Z non-melting material is preferred for initial ITER operation, CFC is therefore the design choice as plasma-facing material at the divertor strike point.

6. Variation in transient frequency

In Fig. 5, the remaining armour thickness of CFC is plotted versus the number of shots to end-of-life. As the frequency of occurrence of slow transients is varied (1 transient every 10, 5, ... 1 shots), the lifetime is reduced, but more than 4000 shots remain even at the highest transient frequency. The last 17 mm of sacrificial thickness are unaffected by transients (Fig. 5; the surface does not become hot enough for strong evaporation). 4000 shots remain also for the low-power point (not shown). The gain in lifetime by going to 40 mm thickness is significant: 2000–4000 shots.

For beryllium, an increase of transient frequency leads to a catastrophic lifetime reduction (Fig. 6a); only the last 1 mm of sacrificial thickness is unaffected by transients.

For W–3%Re, transients have little effect below 20 mm thickness (no melting, little evaporation), but reduce the lifetime very strongly beyond this (Fig. 6b). Therefore, the maximum thickness is chosen as 20 mm (surface temperature 1400 K rather than 1780 K) since higher thickness leads to little gain in lifetime.

Note that transients beyond the first 10 (beryllium), 20–150 (W–3%Re) or 1000 (CFC) transients are unimportant for the erosion lifetime.

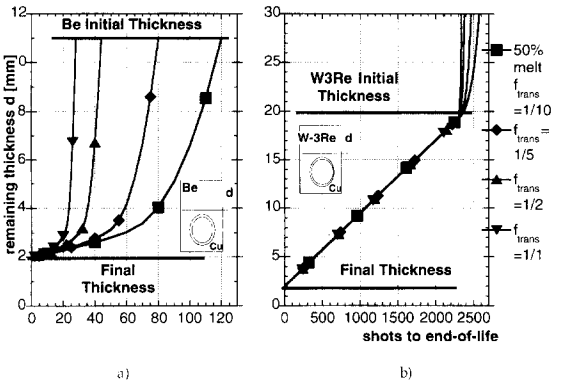

Fig. 6. Remaining Be thickness (a) and W–3%Re thickness (b) with 50% melt loss versus shots to end of life (see Fig. 5).

7. Higher power operation

If the ITER divertor had to be designed for higher-power semi-attached operation, the tile thickness would have to decrease (1080 K limit for Be, 1780 K for CFC and

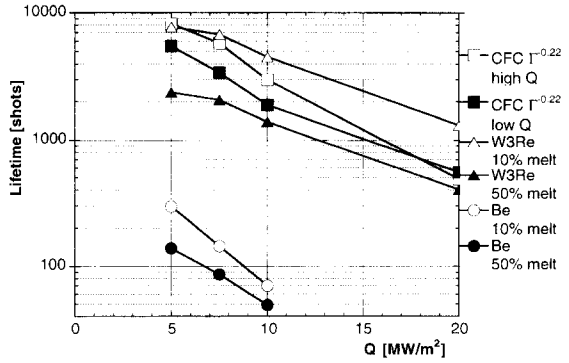

Fig. 7. Composite lifetime for Be, CFC and W–3%Re versus peak power load in normal operation. Melt layer loss varied for metals, lifetime at peak of profile and at lower-power point given for CFC (see text).

W–3%Re except at 5 MW/m^2, see Section 6). More of this power would be carried by particles and T_e at the target would increase. The values taken are shown in Table 2.

The resulting composite lifetime is shown in Fig. 7. The beryllium lifetime is very low and 20 MW/m^2 is not possible. More than 2000 shots for CFC, and 1500–4000 shots for W–3%Re are still obtained at 10 MW/m^2, so that operation with these materials is possible even at higher power.

8. Conclusions

The composite erosion lifetime of the ITER divertor plates for nominal detached operation is determined by physical and chemical sputtering, disruptions and slow transients. For Be, the lifetime is inadequate, 120–320 shots. For W–3%Re, it is 2400–7700 shots, depending on melt layer loss and for CFC it is 5800–8200 shots depending on local power. Even for more frequent slow transients, 4000 shots for CFC and 2300–7800 shots for W–3%Re can still be attained. For semi-attached high-power operation, the thickness decreases, sputtering increases but slow transients are less important, so that the lifetime decreases only by a factor of 2 and both CFC and W–3%Re still reach over 1000 shots.

From the point of view of erosion lifetime of the ITER divertor plates, for high heat flux components near the strike point, Be is excluded but either CFC or W–3%Re can be used. Since a low Z non-melting material is preferred for initial ITER operation, CFC is therefore the design choice at this location.

Acknowledgements

This report has been prepared as an account of work performed under the agreement among the European Atomic Energy Community, the Government of Japan, the Government of the Russian Federation and the Government of the United States of America on Cooperation in the Engineering Design Activities for the International Thermonuclear Experimental Reactor ('ITER EDA Agreement') under the auspices of the International Atomic Energy Agency (IAEA).

References

[1] G. Janeschitz et al., J. Nucl. Mater. 220–222 (1995) 73–88.
[2] ITER JCT and Home Teams, ITER Design Description Document, ITER G 17 DDD 1 94-12-2 W 00-AB, June (1995).
[3] H.D. Pacher et al., NET Internal Note N/I/3330/17/B (1995).
[4] I. Smid, H.D. Pacher et al., Proc. 7th ICFRM, Obninsk, J. Nucl. Mater. (1996), to appear.
[5] R. Matera, G. Federici et al., Proc. 7th ICFRM, Obninsk, J. Nucl. Mater. (1996), to appear.
[6] G. Federici, A.R. Raffray, S. Chiocchio, Yu. Igitkhanov, G. Janeschitz, J. Dietz, H.D. Pacher and I. Smid, Proc. Symp. on Fusion Engineering 95, Champaign, Vol. III (1995).
[7] J.P. Bonal and G. Vieider, private communciation.
[8] W. Eckstein et al., Max-Planck-institut fur Plasmaphysik IPP-9/82 (1993).
[9] G. Federici, D. Holland, J. Brooks et al., Proc. SOFE, Champaign (1995).
[10] C. Garcia-Rosales and J. Roth, Proc. 21st EPS Conf. Controlled Fusion and Plasma Physics, Montpellier (1994) pp. 11–770.
[11] L.D. Horton et al., 15th Int. Conf. on Plasma Physics and Controlled Nuclear Fusion, Sevilla, IAEA, Vienna, Vol. I (1994) p. 541.
[12] H.Y. Guo, J.P. Coad et al., Proc. 22nd EPS Conf. Controlled Fusion and Plasma Phys., Bournemouth, Vol. II (1995) p. 273.
[13] J. Roth et al., Nucl. Fusion, to be published.
[14] B. Goel, H. Wurz et al., KfK 1993 Net Physics Memo NET-PM-94-002 (1994).
[15] L. Lengyel et al., Net Physics Memo NET-PM-94-003 (1994).
[16] A. Sestero et al., Net Physics Memo NET-PM-93-002 (1993).
[17] A. Hassanein and I. Konkashbaev, Nucl. Fusion (Suppl.) 5 (1994) 193.
[18] Yu. Igitkhanov, H.D. Pacher et al., Proc. 22nd EPS Conf. Controlled Fusion and Plasma Physics, Bournemouth, Vol. IV (1995) p. 333.
[19] B.J.D. Tubbing et al., Proc. 22nd EPS Conf. Controlled Fusion and Plasma Physics, Bournemouth, Vol. III (1995) p. 453.
[20] I. Smid, H.D. Pacher et al., NET Internal Note N/I/3330/16/A (1995).